EUROPEAN HEMATOLOGY ASSOCIATION
haematologica
Journal of the European Hematology Association

Germline variants in ETV6 underlie reduced platelet formation, platelet dysfunction and increased levels of circulating CD34+ progenitors

by Marjorie Poggi, Matthias Canault, Marie Favier, Ernest Turro, Paul Saultier, Dorsaf Ghalloussi, Veronique Baccini, Lea Vidal, Anna Mezzapesa, Nadjim Chelghoum, Badreddine Mohand-Oumoussa, Céline Falaise, Rémi Favier, Willem H. Ouwehand, Mathieu Fiore, Franck Peiretti, Pierre Emmanuel Morange, Noémie Saut, Denis Bernot, Andreas Greinacher, Alan T. Nurden, Paquita Nurden, Kathleen Freson, David-Alexandre Trégouët, Hana Raslova, and Marie-Christine Alessi

Haematologica 2016 [Epub ahead of print]

Citation: Poggi M, Canault M, Favier M, Turro E, Saultier P, Ghalloussi D, Baccini V, Vidal L, Mezzapesa A, Chelghoum N, Mohand-Oumoussa B, Falaise C, Favier R, Ouwehand WH, Fiore M, Peiretti F, Morange PE, Saut N, Bernot D, Greinacher A, Nurden AT, Nurden P, Freson K, Trégouët D-A, Raslova H, and Alessi M-C. Germline variants in ETV6 underlie reduced platelet formation, platelet dysfunction and increased levels of circulating CD34+ progenitors. Haematologica. 2016; 101:xxx doi:10.3324/haematol.2016.147694

Germline variants in *ETV6* underlie reduced platelet formation, platelet dysfunction and increased levels of circulating CD34$^+$ progenitors

Marjorie Poggi,[1,*] Matthias Canault,[1,*] Marie Favier,[1,2,*] Ernest Turro[3,4,*], Paul Saultier, [1] Dorsaf Ghalloussi,[1] Veronique Baccini,[1] Lea Vidal,[1] Anna Mezzapesa,[1] Nadjim Chelghoum,[5] Badreddine Mohand-Oumoussa,[5] Céline Falaise,[6] Rémi Favier,[7] Willem H. Ouwehand,[3,8] Mathieu Fiore,[6,9] Franck Peiretti,[1] Pierre Emmanuel Morange,[1,6] Noémie Saut,[1,6] Denis Bernot,[1] Andreas Greinacher[10], NIHR BioResource[11], Alan T. Nurden,[12] Paquita Nurden,[6,12] Kathleen Freson[13,*], David-Alexandre Trégouët,[14,15,16,*] Hana Raslova[2,*] and Marie-Christine Alessi[1,6,*]

[1]*Inserm, UMR 1062, Inra, UMR 1260, Aix Marseille Université, 13005 Marseille, France*

[2]*Inserm U1170, Gustave Roussy, University Paris Sud, Equipe labellisée Ligue contre le Cancer 94805 Villejuif, France*

[3]*Department of Haematology, University of Cambridge, Cambridge CB2 0PT, United Kingdom; National Health Service Blood & Transplant, Cambridge, United Kingdom.*

[4]*MRC Biostatistics Unit, Cambridge, UK*

[5]*Post-Genomic Platform of Pitié-Salpêtrière (P3S), Pierre and Marie Curie University, F-75013 Paris, France*

[6]*French Reference-Center on Inherited Platelet Disorders, France*

[7]*Assistance Publique-Hôpitaux de Paris, Hôpital Armand Trousseau, Paris ; France*

[8]*Wellcome Trust Sanger Institute, Wellcome Trust Genome Campus, Hinxton, Cambridge, United Kingdom.*

[9]*Laboratoire d'hématologie, CHU de Bordeaux, Pessac, France*

[10] *Institute for Immunology and Transfusion Medicine, University Medicine Greifswald, Greifswald 17475, Germany*

[11]*NIHR BioResource - Rare Diseases, Cambridge University Hospitals, Cambridge Biomedical Campus, Cambridge, United Kingdom*

[12]*LIRYC, Plateforme Technologique et d'Innovation Biomédicale, Hôpital Xavier Arnozan, Pessac, France*

[13]*Department of Cardiovascular sciences, Center for Molecular and Vascular Biology, KU Leuven, Belgium*

[14]*ICAN Institute for Cardiometabolism and Nutrition, F-75013 Paris, France*

[15]*Inserm, UMR_S 1166, Team Genomics and Pathophysiology of Cardiovascular Diseases, F-75013 Paris, France*

[16]*Sorbonne Universités, Université Pierre et Marie Curie (UPMC Univ Paris 06), UMR_S 1166, F-75013 Paris, France*

* These authors contributed equally to this work

Running head: ETV6 and platelet formation

Corresponding author: Marie-Christine Alessi, NORT UMR Inserm 1062, Faculté de Médecine Timone 27, Bd Jean Moulin 13385 Marseille, France. E-mail: marie-christine.alessi@univ-amu.fr. Tel: +33 491 324 506; Fax: +33 491 782 101.

Conflict of interest statement: the authors have no conflict of interest to disclose**.**

Word count (abstract): 248
Word count (main text): 3851
Table number: 1
Figure number: 7
Supplemental data: 1

Acknowledgements

Bioinformatics analyses benefit from the C2BIG computing centre funded by the Région Ile de France and UPMC. This work was partially supported by the ICAN Institute for Cardiometabolism and Nutrition (ANR-10-IAHU-05), the Ligue nationale contre le cancer (Labelled team H Raslova), and the "Fondation pour la recherche médicale FRM" (grant to PS FDM20150633607). We thank Dr. J. Ghysdael and Dr. F. Guidez for providing the plasmid constructs, Laboratory of Pr. D. Raoult (URMITE), microscopy unit (P. Weber), Dr Paola Ballerini (Hopital Trousseau) for genotyping; Dr. JC. Bordet for transmission electron microscopy; Dr C Chomiene and C Dosquet for the platelet survival assay; M Crest for experimental help, the French reference center on hereditary platelet disorders (CRPP) for patients' clinical exploration. For the F2-F6 families, study makes use of whole genome sequencing data and analysis approaches generated by the NIHR BioResource - Rare Disease BRIDGE Consortium. The NIHR BioResource - Rare Diseases is funded by the National Institute for Health Research of England (NIHR, www.nihr.ac.uk; award number RG65966). KF is supported by the Fund for Scientific Research-Flanders (FWO-Vlaanderen, Belgium, G.0B17.13N] and by the Research Council of the University of Leuven (BOF KU Leuven, Belgium, OT/14/098].

Abstract

Variants in *ETV6*, which encodes a transcription repressor of the E26 transformation-specific family, have recently been reported to be responsible for inherited thrombocytopenia and hematologic malignancy. We sequenced the DNA from cases with unexplained dominant thrombocytopenia and identified six likely pathogenic variants in *ETV6*, of which five are novel. We observed low repressive activity of all tested ETV6 variants and variants located in the E26 transformation-specific binding domain (encoding p.A377T, p.Y401N) led to reduced binding to co-repressors. We also observed large expansion of CFU-MKs derived from variant carriers and reduced proplatelet formation with

abnormal cytoskeletal organization. The defect in proplatelet formation was also observed in control $CD34^+$ cell-derived megakaryocytes transduced with lentiviral particles encoding mutant ETV6. Reduced expression levels of key regulators of the actin cytoskeleton Cdc42 and RhoA were measured. Moreover, changes in the actin structures are typically accompanied by a rounder platelet shape with a highly heterogeneous size, decreased platelet arachidonic response, spreading and retarded clot retraction in ETV6 deficient platelets. Elevated numbers of circulating $CD34^+$ cells were found in p.P214L and p.Y401N carriers, and two patients from different families suffered from refractory anemia with excess blasts while one patient from a third family was successfully treated for acute myeloid leukemia. Overall, our study provides novel insights into the role of ETV6 as a driver of cytoskeletal regulatory gene expression during platelet production and the impact of variants resulting in platelets with altered size, shape and function and potentially also in changes in circulating progenitor levels.

Introduction

The genetic determinants of non-syndromic autosomal dominant (AD) thrombocytopenia with normal platelet size remains largely unknown, yet it is important to identify such variants because they may predispose carriers to hematological malignancy. Germline variants in *RUNX1* cause a familial platelet disorder with increased risk of acute leukemia (FPD/AML) while variants in the 5′ untranslated region (UTR) of *ANKRD26* have also been shown to predispose individuals to hematologic malignancies. Recently, germline variants in *ETV6 (TEL)* have been reported to underlie AD thrombocytopenia with predisposition to leukemia.[1-3] *ETV6*, which was initially identified as encoding a tumor suppressor in humans, is often found fused with partner genes in samples from human leukemia of myeloid and lymphoid origin.[4] Somatic *ETV6* variants have also been found in solid tumors, T-cell leukemias and myelodysplastic syndromes, hence the widespread interest in this gene.[5,6] *ETV6* encodes an E26 transformation-specific (Ets) family transcription repressor. It can bind DNA via a highly conserved Ets DNA-binding consensus site located at the C-terminus. The N-terminal domain (pointed domain) is necessary for homotypic dimerization and interaction with the Ets family protein FLI.[7,8] The central region is involved in repression complex recruitment (including SMRT, mSin3A and N-CoR)[9] and autoinhibitory activity.[10]

ETV6 plays an important role in hematopoiesis. In mice, ETV6 is essential for hematopoietic transition from the fetal liver to the bone marrow (BM).[11] Conditional disruption of the *ETV6* gene has shown that ETV6 plays a unique, non-redundant role in megakaryocytopoiesis. Data concerning ETV6 involvement in megakaryocytopoiesis in humans remains scarce, however, a recent study has shown that patients expressing a mutated form of ETV6 displayed abnormal megakaryocyte (MK) development with a likely impact on platelet production.[1]

We have assessed the biological impact of six likely pathogenic variants in *ETV6*, of which five are novel. We describe in detail how variants in *ETV6* lead to increased MK proliferation and various cytoskeleton-related platelet defects that include altered platelet shape, reduced Rho-GTPase expression in platelets, decreased proplatelet formation and reduced platelet spreading. Additionally, we show that patients exhibit elevated levels of circulating $CD34^+$ progenitors and predisposition to myelodysplastic syndrome and leukemia.

Methods

Platelets and circulating CD34$^+$-cells analysis

Blood samples were collected after informed written consent, in accordance with our local Institutional Review Boards and the Declaration of Helsinki. Platelet-rich plasma (PRP), washed platelets and circulating CD34$^+$-cells were prepared according to standard procedures. For electron microscopy (EM), platelets were fixed in glutaraldehyde and processed as previously described[12]. For platelet spreading, fibronectin-adherent platelets were stained with Alexa 488-phalloidin (F-actin) and Alexa 594-DNAse I (G-actin). Filopodia and lamellipodia were manually quantified. For clot retraction, coagulation of PRP was triggered using thrombin, and clots were allowed to retract. Images were recorded using a CoolSNAP CCD-camera and analyzed to evaluate the reduction of the initial clot surface (ImageJ). The platelet survival assay was based on the method of Thakur *et al.*.[13]

High-throughput and Sanger sequencing

DNA samples from 957 patients enrolled to the BRIDGE-BPD project were subjected to whole-genome or whole-exome sequencing and the results were used for variant calling as described previously.[14,15] DNA samples from 8 patients in the French collection were subjected to whole-exome sequencing and analyzed using Chromas software or Sanger sequencing at the *ETV6* locus and analyzed with Multalign.[16]

Site-directed mutagenesis and luciferase assays

ETV6 cDNA was ligated into a pcDNA3 expression vector, and mutagenesis was performed using the GENEART® Site-directed Mutagenesis System kit (Life technologies)[17]. Transcriptional regulatory properties of wild-type (wt) and mutant ETV6 (mutETV6), as well as ETV6 co-repressor binding[18], were determined by using the luciferase reporter systems in transfected GripTite™ 293 MSR cells.

Immunoassays

Immunoblots were performed with antibodies directed against human ETV6, SMRT, RhoA (Santa Cruz), Cdc42, Rac1 and GAPDH (Millipore) and MYH10 (Cell Signaling Technology) antibodies. Chemiluminescence signals were detected and quantified (CCD camera-based ImageQuant LAS 4000, GE Healthcare). Levels of thrombopoietin (TPO) and stromal cell-derived factor 1 (SDF1α) were quantified via ELISA (Abcam). For the co-immunoprecipitation assays, whole cell extracts were prepared in NP-40 buffer and pre-cleared with protein A/G magnetic beads (Millipore). Immunoprecipitation of the cell extracts with anti-ETV6-coated beads was carried out overnight.

MK differentiation and quantification of proplatelet-bearing MKs

$CD34^+$-cells were grown in serum-free medium supplemented with TPO and Stem Cell Factor (SCF) (Life Technologies)[19]. At culture day 10, we assessed ploidy in the $Hoechst^+CD41^+CD42a^+$ cell population[20] (Navios, BD Biosciences). Proplatelets were quantified between day 11 and 15. Microtubule and F-actin organization was determined in MKs adhering to fibrinogen with fluorescently labeled polyclonal rabbit anti-tubulin antibody (Sigma-Aldrich) and phalloidin (Life Technologies).

Lentiviral particle production and $CD34^+$ cell transduction

Lentiviral particles were prepared as previously described.[21,22] $CD34^+$ cells were infected twice. After 8 hours, the cells were washed and cultured in serum-free medium.

Clonogenic progenitor assays

$CD34^+$-cells were plated in human methylcellulose medium H4434 (STEMCELL Technologies) supplemented with EPO, IL-3, SCF, G-CSF, IL6 and TPO to quantify erythroid (BFU-E, CFU-E), granulocytic/macrophage (CFU-GM), mixed (CFU-GEMM) and megakaryocyte (CFU-MK) progenitors at day 12.[23]

Statistical analyses

Analyses were performed using GraphPad Prism software. Statistical significance was determined via a 2-tailed Mann-Whitney test. $P<0.05$ was considered statistically significant.

Results

Identification of affected families

Screening of patients with thrombocytopenia for rare non-synonymous variants in *ETV6* revealed six families with patients carrying one of six possibly pathogenic variants. The variants encode p.P214L, which has been previously reported[3], and the novel substitutions p.I358M, p.A377T, p.R396G, p.Y401N and p.Y401H (Figure 1a). Family studies by Sanger sequencing showed segregation between the ETV6 variant and thrombocytopenia in all cases for which DNA samples were available (Figure 1b). Henceforth, we refer to the likely pathogenic variants described above as mut*ETV6*.

Description of the families

Our study includes six families with mut*ETV6* variants. The proband of the first family (F1-IV3) is a 7-year-old girl who was admitted for emergency care due to suspicion of acute leukemia with asthenia, weakness, paleness, severe thrombocytopenia (44 x 10^9/L) and anemia (hemoglobin: 50 g/L). BM examination unequivocally dismissed a diagnosis of leukemia, and the anemia was attributed to an iron deficiency subsequent to repeated episodes of severe epistaxis. The patient underwent a red blood cell transfusion, and the anemia was progressively corrected via iron supplementation. However, the platelet count remained low (50 x 10^9/L). Clinical examination of the parents and two siblings did not reveal any particular bleeding tendency. However, the patient's mother (F1-III3) had undergone a splenectomy at the age of 17 because of chronic thrombocytopenia, and she exhibited subnormal platelet counts (116-210 x 10^9/L) at the time of examination. To gain further insight into the possibility of inherited thrombocytopenia, we screened the extended family for platelet counts. An AD form of thrombocytopenia was evidenced (Figure 1b) with normal Mean Platelet Volume (MPV) compared with a large population of blood donors (figure 1c). Of note 14 over 23 carriers exhibit MPV >9 fL (Table). Plasmatic TPO levels were decreased in affected F1 members (n=4): 160 ± 9 pg/mL vs. controls (n=8): 296 ± 39 pg/mL, p=0.02). May-Grünwald Giemsa staining of BM smears of patients F1-IV3 showed that MKs were present, although a high proportion was of medium size in the early stages of maturation and tend to be hypolobulated (Figure 1d). The 7-year-old patient's grandfather (F1-II2) was diagnosed with refractory anemia with excess blasts type 2 (RAEB-2) at the age of 70. Individuals from the second and third families had platelet counts between 60 and 125 x 10^9/L (Table). BM from F2-II3 displayed a delay in granulocyte maturation and dyserythropoiesis (data not shown). Peripheral blood smears revealed platelet anisocytosis (data not shown) as confirmed via electron microscopy (Figure 1e), which further highlighted the presence of occasional hypogranular platelets with a poorly organized open canalicular system. Patient F2-I1 presented with RAEB and required BM transplantation. The propositus (F4-II1) from pedigree 4 was referred with acute myeloid leukemia (AML)-type M0 at the age of 8 years and suffered from epistaxis, ecchymosis and infections. After 2 years of chemotherapy treatment, the bone marrow showed no blasts and the peripheral blood counts normalized except for a persistent low platelet count (Table). Bone marrow studies showed the

presence of many hypolobulated small MKs (data not shown). Thrombocytopenia was also present in his father and two sisters without any bleeding problems (Table). EM investigation of platelets from affected members F4-I2 and F4-II3 showed the presence of both larger and smaller platelets that were significantly of round shape rather than of discoid shape (Figures 1e and 1f; $p<0.0001$). These platelets have normal dense and alpha granules numbers but some alpha granules are elongated (data not shown). Pedigree 5 was referred for genetic testing of AD thrombocytopenia in a father with very mild bleeding problems (propositus F5-I2) and his 2 asymptomatic daughters (Figure 1b). Bone marrow investigation in F5-II2 showed the presence of dysmegakaryopoiesis with almost no mature MKs (data not shown). A mother (F6-I1) and daughter (propositus F6-II1) from pedigree 6 (Figure 1b) were diagnosed with platelet dense storage pool deficiency (SPD) with platelet aggregation defects and abnormal dense granules. Thrombocytopenia was only recorded for the daughter who suffered from severe menorrhagia and has an increased bleeding tendency with bruising and nosebleeds. The mother has a normal platelet count and did not carry the ETV6 variant. No clinical information or DNA was available from the father. Therefore, the ETV6 variant in F6-II1 can be present as a *de novo* or somatic variant. SPD in the mother and daughter is likely to be caused by another additional genetic factor. Indeed, in contrast to the obvious platelet aggregation and secretion defects for these two patients, such abnormalities were not present in the other 5 families except for a decreased aggregation response to arachidonic acid as the only consistent finding in every family (supplemental table 1). Consistent with normal dense granules found by EM (Figure 1e), ATP secretion and mepacrine uptake and release were normal (Supplemental Table 1). Flow cytometry analysis of key platelet surface receptors ($\alpha_{IIb}\beta_3$, glycoprotein (GP) Ibα, GPIa, GPIV, CD63 and CD62P) was also normal (Supplemental Table 2).

A platelet survival assay was performed (patient F3-II4) (Supplemental Table 3) and revealed decreased platelet lifespan (4.6 days) without significant splenic or hepatic sequestration. Notably, this patient had not undergone platelet transfusion. Patient F1-III3 underwent a ^{111}In-oxine platelet survival assessment (autologous transfusion) in 1981 prior to splenectomy, which revealed short platelet half-life (24 h vs. 3.5 days in the control) and hepatic and splenic platelet sequestration, with predominant sequestration in the liver (data not shown). Patient F1-III3 was assessed for anti-HLA antibodies on several occasions (National Center of Blood Transfusion, Marseille), but all results were negative (data not shown).

Variants in *ETV6* lead to a functional defect in transcriptional activity

Western blot analysis showed that ETV6 protein expression was not reduced in platelets from the patients, nor in GripTite™ 293 MSR cells transfected with the *ETV6* variants (Figures 2a and 2b). To investigate the transcriptional regulatory properties of mutETV6 compared with wtETV6, we analyzed repressive activity. Co-transfection of the reporter plasmid along with expression of a plasmid encoding wtETV6 resulted in almost 90% inhibition of luciferase activity. Substitution of wtETV6 with

any of the mutETV6 variants led to a significant reduction in repressive activity (85% to 100%) (Figure 2c).

To evaluate whether this reduction in repressive activity may result from variations in nuclear co-repressor complex recruitment, we investigated the interaction of ETV6 with N-CoR, SMRT and Sin3A using a mammalian 2-hybrid assay. p.P214L ETV6 interacted with N-CoR, SMRT and mSin3A, whereas p.A377T and p.Y401N ETV6 did not (Figure 3d). Immunoprecipitation assays showed that the p.A377T and p.Y401N variants reduced ETV6 binding to SMRT and SMRTe (Figure 3e).

Increased numbers of circulating CD34 positive cells in affected family members

F1 carriers (F1-III3, F1-III7, F1-III8, F1-IV1 and F1-IV3) exhibited a 4- to 6-fold increase in circulating $CD34^+/CD38^+$ cells compared with healthy donors (Figures 3a and 3b). Similarly, F3-I2 and F3-II4 exhibited a 5- and 3-fold increase in circulating CD34+ cells compared with controls (0.16% and 0.09%, respectively, vs. 0.035%). The expression levels of immature cell markers CD133 and CD117 did not differ between F1 members and controls. Expression of the myeloid lineage marker CD33 contrasted with the absence of MK lineage markers CD123, CD41, CD61 and CD42b (data not shown). Additionally, plasma levels of SDF-1α did not vary between patients (F1: 1966 ± 95 pg/mL; n=8) and controls (2068 ± 75 pg/mL; n=9).

Variants in *ETV6* cause MK hyperplasia but reduced proplatelet formation *in vitro*

The percentage of $CD41^+CD42a^+$ MKs derived from $CD34^+$ (gated on $Hoechst^+$ cells) was significantly higher in mut*ETV6* carriers (Figures 4a and 4b). No significant difference in mean ploidy was detected between patients and healthy donors (Figure 5c). Accordingly, the number of $CD34^+$-derived CFU-GM/G/M colonies was higher in patients compared with controls (Figure 4d). The number of MK progenitors (CFU-MK) from patients F3-I2 and F3-II4 did not differ from controls, although the size of CFU-MKs was significantly increased in the two patients (Figures 4e and 4f), thereby suggesting increased proliferation of MK precursors in the presence of *mutETV6*.

Proplatelet (PPT)-bearing MKs derived from controls showed multiple branched thin extensions, swellings and tips. In contrast, MKs from patients formed very few PPTs with a reduced number of thicker extensions. Although there was no swelling, tips were of increased size (Figure 5a). A two- to fifteen-fold decrease in the percentage of PPT-bearing MKs was observed in carriers of the p.P214L (F1-III3, F1-III7 and F1-IV3) and p.Y401N (F3-II2 and F3-II4) variants (Figure 5b). β-tubulin and F-actin staining confirmed the MK-PPT extension defect together with a reduced concentration of both actin filaments and microtubules in the residual larger MK cell body (Figure 5c). Additionally, β-tubulin failed to accumulate normally in the few extension tips observed in mutETV6 MKs compared with controls.

To confirm that *mutETV6* leads to a defect in PPT formation, $CD34^+$ cells from healthy donors were transduced with lentivirus containing *ETV6* sequences encoding the wt or the p.P214L mutant. Non-transduced cells were also included as control. After 13 and 15 days of culture in the presence of TPO and SCF, cells transduced with mut*ETV6* lentivirus did not form PPTs, in contrast to non-transduced cells or those transduced with wt *ETV6* (Figure 5d).

mutETV6 does not alter MYH10 expression but was associated with decreased expression and activity of the key regulators of the actin cytoskeleton Cdc42 and RhoA

To assess potential cooperation between the ETV6, RUNX1 and FLI1 pathways we examined MYH10 protein expression levels in patient platelets. We did not detect increased MYH10 levels in platelets from ETV6 patients (F1-III6 and F1-III8), which contrasted with *RUNX1* and *FLI1* defects[24] (Supplemental Figures 1a and 1b).

PPT formation is dependent on massive reorganization of the actin cytoskeleton. Rho-GTPase family members (e.g., Cdc42, Rac1 and RhoA) are key regulators of actin cytoskeleton dynamics in platelets[25] and MKs. p.P214L (n=5) and p.Y401N (n=2) variants led to significantly reduced platelet expression levels of Cdc42 and RhoA, without affecting Rac1 expression (Figure 6a). Likewise, Cdc42 and RhoA mRNA levels were decreased in MKs from F1 and F3, while Rac1 mRNA levels remained unaffected (Figure 6b). Notably, patient F3-I2, with 112 x 10^9 platelets/L, exhibits only slightly decreased levels of Cdc42 and RhoA in platelets (Figure 6c) compared with other affected members. Cdc42 and RhoA levels significantly correlated with platelet count (n=6 from F1 and F3) ($p=0.03$ and $r=0.84$ for Cdc42; $p=0.008$ and $r=0.92$ for RhoA). To confirm the specificity of this effect, we quantified Cdc42 protein levels in *FLI1* deficient patients with thrombocytopenia (n=2) (122 and 131 x 10^9/L). None of these patients exhibited reduced levels of Cdc42 (Supplemental Figure 1c).

Overexpression of Cdc42 in $CD34^+$-derived MKs from patients (F1-III3, F1-III7, F1-III8) did not fully reverse the phenotype, although it did improve the PPT-bearing MK phenotype. Transduced cells produced thinner extensions and swellings, which were not observed in control transduced cells (Figure 6d).

***mutETV6* alters platelet spreading**

Reduced expression of Cdc42 and RhoA suggests that ETV6 is involved in cytoskeletal reorganisation that thus not only having an important role in platelet shape (EM showed more round platelets) and proplatelet formation but also in regulating platelet spreading. We assessed whether the p.P214L transition in ETV6 affects spreading of platelets over immobilized fibronectin and clot retraction. Platelets showed reduced capacity to form filopodia and lamellipodia, under unstimulated and ADP-stimulated conditions, respectively (Figure 7a). The G/F actin ratio was significantly higher in the rare patient platelets that spread (Figure 7b). Furthermore, reduced clot retraction velocity was noticeable

in the mutant (Figure 7c).

Discussion

Here, we present six families with AD thrombocytopenia associated with germline variants in *ETV6*. $CD34^{+}$-derived MKs from mut*ETV6* carriers showed a reduced ability to form PPTs. The variants in the ETS domain impaired interaction with the co-repressors N-COR, SMRT and Sin3B. Patient platelets are more round and have a reduced capacity to form filopodia and lamellipodia, which was associated with reduced expression levels of cytoskeletal regulators Cdc42 and RhoA. Additionally, mutETV6 carriers displayed increased numbers of circulating $CD34^{+}$ progenitor cells, which may contribute to predisposition to hematologic malignancy.

Loss of ETV6 function has been reported to contribute to leukemia, predominantly due to somatic variants and fusion transcripts.[3] Four amino acid substitutions described in this study are listed in the catalog of somatic mutations in cancer (COSMIC). The p.P214L, p.R396G and p.A377T variants were present in digestive tract tumors[26] while p.Y401C has been associated with acute myeloid leukemia.[27] More recently, also germline *ETV6* variants have been found to predispose to cancer. Eleven patients carrying *mutETV6* (p.P214L, p.R399C, p.R369Q, p.L349P, p.N385fs or p.W380R) developed acute lymphocytic leukemia or myelodysplastic syndrome.[1-3,28] Two affected members of the families F1 and F2 had myelodysplasia with RAEB and one of the F4 family was successfully treated with chemotherapy for AML-M0.

Variants reduced the repressive activity of ETV6 without altering ETV6 protein expression levels in platelets. Alteration of ETV6 repressive activity can be explained by modification of ETV6 cellular localization, as p.P214L and four other variants affecting the ETS domain lead to ETV6 sequestration in the cytoplasm in both HeLa transfected cells and cultured MKs.[1-3] However, three of these variants only partially prevented nuclear localization, thereby indicating other possible mechanisms. The p.A377T and p.Y401N variants prevented co-repressor complex recruitment. These substitutions are located in the ETV6 Ets second and third alpha helix, contiguous to amino acids involved in key hydrophobic contacts with the H5 helix of the C-terminal inhibitory domain (aa 426-436)[29] thus possibly affecting ETV6 DNA-binding ability. In immunoprecipitation assays, overexpression of wt or p.P214L ETV6 did not modify the interaction between SMRT and ETV6, while p.A377T and p.Y401N ETV6 significantly reduced this interaction. Overall, this suggests that variants in the Ets DNA-binding domain exert a dominant negative effect.

ETV6 has been shown to drive MK differentiation of hematopoietic stem cells.[30] From literature and supported by bone marrow studies in F4-II1 and F5-II2, ETV6 defects seem to result in an increased percentage of small MKs[1]. Our MK colony assays confirmed an increased proliferation of early MK progenitors characterized by increased production of $CD41^{+}CD42a^{+}$ MKs compared to control conditions. This may explain the reduced TPO levels observed in the affected members of family F1. Accordingly, loss of ETV6 in the erythro-megakaryocytic lineage in mice also results in large, highly proliferative early MKs and mild thrombocytopenia. We cannot exclude that ETV6-driven deregulation

of MK proliferation may take place in hematopoietic progenitors, thereby promoting oncogenic transformation. Altogether, these data do not support the concept that signaling between the ETV6 and RUNX1/FLI1/ANKRD26 pathways is involved in the underlying mechanism, as variants in these genes were associated with a decreased or normal MK colony formation.[19,31,32] Furthermore, MYH10 expression levels remained low in patients with *mutETV6*, which indicates unaltered RUNX1 and FLI1 function.[24]

Despite the increased early MK proliferation potential, $CD34^+$-derived MKs from patients with mut*ETV6* showed reduced capacity to form PPTs. These altered MK features suggest that a defect in cytoskeletal reorganization during PPT formation likely causes thrombocytopenia in patients. Sequencing of platelet RNA from patients with p.P214L ETV6 revealed a considerable reduction in the levels of several cytoskeletal transcripts.[1] Furthermore, Palmi *et al*[33] showed that the ETV6-RUNX1 fusion protein, which is associated with a loss of ETV6 repressive activity[34,35], alters the expression of genes regulating cytoskeletal organization. In particular, the ETV6-RUNX1 fusion protein led to reduced expression of Cdc42. The mechanism by which the loss of ETV6 repressive activity results in reduced Cdc42 and RhoA expression remains to be resolved.

Cdc42 is an important mediator of platelet and MK cytoskeleton reorganization.[36] Therefore, we hypothesize that ETV6 repressive activity is a key regulator of MK cytoskeleton remodeling driven via Rho-GTPases in mutETV6 carriers. *mutETV6* was associated with a decrease in Cdc42 and RhoA expression levels in platelets without affecting Rac1 expression. Additionally, mutETV6 platelets showed defects in functions classically associated with Cdc42 (i.e., filopodia formation) and RhoA (i.e., lamellipodia formation and clot retraction).[36] Electron microscopy also showed platelets of variable sizes and having a more round instead of discoid shape. RNA sequencing previously performed on mutETV6 transfected cells, patient platelets and leukemia cells did not reveal any modification in Rho-GTPase mRNA levels[1,3], which may be due to variations in the models applied. Indeed, Rho-GTPase mRNA levels were evaluated in $CD34^+$-derived MKs, and the reduced mRNA levels were confirmed at the protein level in patient platelets. Moreover, we observed a correlation between platelet count and Cdc42 and RhoA expression levels, thereby suggesting a relationship between thrombocytopenia severity and Rho-GTPase levels. Key regulators of the actin cytoskeleton Cdc42 and RhoA have already been shown to be associated with thrombocytopenia due to defects in cytoskeleton organization.[37-41] In affected individuals, we found abnormal tubulin organization in PPT-forming MKs and altered actin polymerization in platelets. Rescue experiments with Cdc42 lentiviral particles were not able to fully reverse the phenotype, although the cells produced thinner extensions and swellings, which were barely observed in control cells.

In mice, Cdc42 or RhoA deficiency causes increased platelet clearance.[37,38] Such an observation was noted in two patients: one young girl who never received platelets (F3-II4) and a patient for whom splenectomy improved the platelet count (F1-III3). This suggests that ETV6 mutations are linked to

several defects with reduced platelet formation and survival, although this latter mechanism requires further confirmation.

Individuals carrying a germline ETV6 variant showed increased numbers of circulating $CD34^+/CD133^+$cells. The phenotype of these stem cells did not differ between patients and controls. This increase has to be considered as a helpful marker of the ETV6-related thrombocytopenia. It may not be attributed to excessive proliferation, as Zhang *et al.* showed reduced proliferation of $CD34^+$ cells expressing wt or mutETV6.[3] Interestingly, the defect in Cdc42 expression may also account for increased hematopoietic progenitor mobilization, as chemical inhibition of Cdc42 in mice efficiently improved progenitor recruitment in the peripheral blood. Altered interaction between mutated progenitors and the BM microenvironment, as reported in the case of the ETV6-RUNX1 fusion protein, may also be involved.[33] Further investigations are required to more precisely delineate the role that ETV6 plays in stem cell progenitor mobilization.

In conclusion, we identified 6 variants in ETV6, of which 5 are novel, associated with dominant thrombocytopenia. Our study provides novel insights into the role that ETV6 plays in platelet function, morphology and formation that seem all driven by changes in the cytoskeleton and potentially also in circulating $CD34^+$ progenitor levels.

References

1. Noetzli L, Lo RW, Lee-Sherick AB, et al. Germline mutations in ETV6 are associated with thrombocytopenia, red cell macrocytosis and predisposition to lymphoblastic leukemia. Nat Genet. 2015;47(5):535-538.
2. Topka S, Vijai J, Walsh MF, et al. Germline ETV6 Mutations Confer Susceptibility to Acute Lymphoblastic Leukemia and Thrombocytopenia. PLoS Genet. 2015;11(6):e1005262.
3. Zhang MY, Churpek JE, Keel SB, et al. Germline ETV6 mutations in familial thrombocytopenia and hematologic malignancy. Nat Genet. 2015;47(2):180-185.
4. Rowley JD. The critical role of chromosome translocations in human leukemias. Annu Rev Genet. 1998;32:495-519.
5. Bejar R, Stevenson K, Abdel-Wahab O, et al. Clinical effect of point mutations in myelodysplastic syndromes. N Engl J Med. 2011;364(26):2496-2506.
6. Van Vlierberghe P, Ambesi-Impiombato A, Perez-Garcia A, et al. ETV6 mutations in early immature human T cell leukemias. J Exp Med. 2011;208(13):2571-2579.
7. Kwiatkowski BA, Bastian LS, Bauer TR, Jr., Tsai S, Zielinska-Kwiatkowska AG, Hickstein DD. The ets family member Tel binds to the Fli-1 oncoprotein and inhibits its transcriptional activity. J Biol Chem. 1998;273(28):17525-17530.
8. Chakrabarti SR, Sood R, Ganguly S, Bohlander S, Shen Z, Nucifora G. Modulation of TEL transcription activity by interaction with the ubiquitin-conjugating enzyme UBC9. Proc Natl Acad Sci U S A. 1999;96(13):7467-7472.
9. Wang L, Hiebert SW. TEL contacts multiple co-repressors and specifically associates with histone deacetylase-3. Oncogene. 2001;20(28):3716-3725.
10. Green SM, Coyne HJ, 3rd, McIntosh LP, Graves BJ. DNA binding by the ETS protein TEL (ETV6) is regulated by autoinhibition and self-association. J Biol Chem. 2010;285(24):18496-18504.
11. Wang LC, Swat W, Fujiwara Y, et al. The TEL/ETV6 gene is required specifically for hematopoiesis in the bone marrow. Genes Dev. 1998;12(15):2392-2402.
12. Nurden P, Debili N, Vainchenker W, et al. Impaired megakaryocytopoiesis in type 2B von Willebrand disease with severe thrombocytopenia. Blood. 2006;108(8):2587-2595.
13. Thakur ML, Walsh L, Malech HL, Gottschalk A. Indium-111-labeled human platelets: improved method, efficacy, and evaluation. J Nucl Med. 1981;22(4):381-385.
14. Westbury SK, Turro E, Greene D, et al. Human phenotype ontology annotation and cluster analysis to unravel genetic defects in 707 cases with unexplained bleeding and platelet disorders. Genome Med. 2015;7(1):36.
15. Turro E, Greene D, Wijgaerts A, et al. A dominant gain-of-function mutation in universal tyrosine kinase SRC causes thrombocytopenia, myelofibrosis, bleeding, and bone pathologies. Sci Transl Med. 2016;8(328):328ra330.
16. Barton GJ, Sternberg MJ. A strategy for the rapid multiple alignment of protein sequences. Confidence levels from tertiary structure comparisons. J Mol Biol. 1987;198(2):327-337.
17. Lopez RG, Carron C, Oury C, Gardellin P, Bernard O, Ghysdael J. TEL is a sequence-specific transcriptional repressor. J Biol Chem. 1999;274(42):30132-30138.
18. Guidez F, Petrie K, Ford AM, et al. Recruitment of the nuclear receptor corepressor N-CoR by the TEL moiety of the childhood leukemia-associated TEL-AML1 oncoprotein. Blood. 2000;96(7):2557-2561.
19. Bluteau D, Balduini A, Balayn N, et al. Thrombocytopenia-associated mutations in the ANKRD26 regulatory region induce MAPK hyperactivation. J Clin Invest. 2014;124(2):580-591.
20. Lordier L, Bluteau D, Jalil A, et al. RUNX1-induced silencing of non-muscle myosin heavy chain IIB contributes to megakaryocyte polyploidization. Nat Commun. 2012;3:717.
21. Naldini L, Blomer U, Gallay P, et al. In vivo gene delivery and stable transduction of nondividing cells by a lentiviral vector. Science. 1996;272(5259):263-267.
22. Raslova H, Komura E, Le Couedic JP, et al. FLI1 monoallelic expression combined with its hemizygous loss underlies Paris-Trousseau/Jacobsen thrombopenia. J Clin Invest. 2004;114(1):77-84.
23. Klimchenko O, Mori M, Distefano A, et al. A common bipotent progenitor generates the erythroid and megakaryocyte lineages in embryonic stem cell-derived primitive hematopoiesis. Blood. 2009;114(8):1506-1517.
24. Antony-Debre I, Bluteau D, Itzykson R, et al. MYH10 protein expression in platelets as a biomarker of RUNX1 and FLI1 alterations. Blood. 2012;120(13):2719-2722.

25. Goggs R, Williams CM, Mellor H, Poole AW. Platelet Rho GTPases-a focus on novel players, roles and relationships. Biochem J. 2015;466(3):431-442.
26. Seshagiri S, Stawiski EW, Durinck S, et al. Recurrent R-spondin fusions in colon cancer. Nature. 2012;488(7413):660-664.
27. Dolnik A, Engelmann JC, Scharfenberger-Schmeer M, et al. Commonly altered genomic regions in acute myeloid leukemia are enriched for somatic mutations involved in chromatin remodeling and splicing. Blood. 2012;120(18):e83-92.
28. Melazzini F, Palombo F, Balduini A, et al. Clinical and pathogenetic features of ETV6 related thrombocytopenia with predisposition to acute lymphoblastic leukemia. Haematologica. 2016.
29. Coyne HJ, 3rd, De S, Okon M, et al. Autoinhibition of ETV6 (TEL) DNA binding: appended helices sterically block the ETS domain. J Mol Biol. 2012;421(1):67-84.
30. Sakurai T, Yamada T, Kihara-Negishi F, et al. Effects of overexpression of the Ets family transcription factor TEL on cell growth and differentiation of K562 cells. Int J Oncol. 2003;22(6):1327-1333.
31. Bluteau D, Glembotsky AC, Raimbault A, et al. Dysmegakaryopoiesis of FPD/AML pedigrees with constitutional RUNX1 mutations is linked to myosin II deregulated expression. Blood. 2012;120(13):2708-2718.
32. Breton-Gorius J, Favier R, Guichard J, et al. A new congenital dysmegakaryopoietic thrombocytopenia (Paris-Trousseau) associated with giant platelet alpha-granules and chromosome 11 deletion at 11q23. Blood. 1995;85(7):1805-1814.
33. Palmi C, Fazio G, Savino AM, et al. Cytoskeletal Regulatory Gene Expression and Migratory Properties of B Cell Progenitors are Affected by the ETV6-RUNX1 Rearrangement. Mol Cancer Res. 2014;12:1796-1806.
34. Song H, Kim JH, Rho JK, Park SY, Kim CG, Choe SY. Functional characterization of TEL/AML1 fusion protein in the regulation of human CR1 gene promoter. Mol Cells. 1999;9(5):560-563.
35. Rho JK, Kim JH, Yu J, Choe SY. Correlation between cellular localization of TEL/AML1 fusion protein and repression of AML1-mediated transactivation of CR1 gene. Biochem Biophys Res Commun. 2002;297(1):91-95.
36. Aslan JE, McCarty OJ. Rho GTPases in platelet function. J Thromb Haemost. 2013;11(1):35-46.
37. Pleines I, Eckly A, Elvers M, et al. Multiple alterations of platelet functions dominated by increased secretion in mice lacking Cdc42 in platelets. Blood. 2010;115(16):3364-3373.
38. Pleines I, Hagedorn I, Gupta S, et al. Megakaryocyte-specific RhoA deficiency causes macrothrombocytopenia and defective platelet activation in hemostasis and thrombosis. Blood. 2012;119(4):1054-1063.
39. Suzuki A, Shin JW, Wang Y, et al. RhoA is essential for maintaining normal megakaryocyte ploidy and platelet generation. PLoS One. 2013;8(7):e69315.
40. Pleines I, Dutting S, Cherpokova D, et al. Defective tubulin organization and proplatelet formation in murine megakaryocytes lacking Rac1 and Cdc42. Blood. 2013;122(18):3178-3187.
41. Chen C, Song X, Ma S, et al. Cdc42 inhibitor ML141 enhances G-CSF-induced hematopoietic stem and progenitor cell mobilization. Int J Hematol. 2015;101(1):5-12.

Table 1: Hematological parameters in the six studied family members

Family-Individuals	Gender	ETV6 genotype	Current age	Red cell count	Hyperdense Red blood cells	Hemoglobin	Mean corpuscular hemoglobin concentration	Mean corpuscular volume	Platelet count	Mean platelet volume	Absolute neutrophil count	Absolute lymphocyte count	Absolute monocyte count
Normal range				4.0-5.0 x 10^{12}/L	0.0-2.5 %	115-160 g/L	310-350 g/L	80-100 fL	150-400 x 10^9/L	7.0-9.0 fL	2.0-7.5 x 10^9/L	1.5-4.0 x 10^9/L	0.2-2.0 x 10^9 /L
F1-II1	F	WT	70	5.0	1.1	155	343	89	242	8.4	2.4	**1.2**	0.3
F1-II2	M	P214L	69	**3.3**	**4.3**	117	350	**101**	**44**	7.2	**1.3**	**1.0**	0.2
F1-II4	F	P214L	69	4.5	1.1	144	342	94	**64**	8.0	3.6	**0.8**	0.3
F1-III1	M	WT	53	4.6	1.5	130	340	84	224	**10.2**	4.3	1.6	0.3
F1-III3	F	P214L	43	4.0	0.6	125	323	95	**116**-210	**12.4**	2.9	1.5	0.5
F1-III5	M	P214L	27	4.3	**5.0**	140	**359**	92	**55**	8.8	3.9	**1.0**	0.5
F1-III6	M	P214L	18	4.8	**6.4**	152	**353**	89	**51**	8.4	3.1	**1.4**	0.5
F1-III7	M	P214L	43	4.5	ND	147	ND	94	**58**	**10.6**	4.6	**0.8**	0.6
F1-III8	M	P214L	27	5.0	**2.6**	169	**354**	92	**38**	7.9	2.7	1.8	0.5
F1-IV1	F	P214L	13	4.2	2.0	130	337	91	**85**	8.7	2.3	1.7	0.2
F1-IV2	M	WT	11	5.0	1.7	138	338	81	184	8.5	2.0	2.1	0.2
F1-IV3	F	P214L	8	4.3	**5.7**	131	**354**	83	**50**	**10.2**	**1.6**	1.5	0.2
F2-II2	F	A377T	28	4.9	ND	**162**	342	97	**84**	9.0	4.0	2.0	0.4
F2-II3	M	A377T	24	4.8	ND	**167**	343	**102**	**60**	7.9	3.2	**1.2**	0.5
F2-III1	M	ND	7	4.4	ND	125	330	87	**85**	7.7	**1.6**	2.8	0.5
F2-III2	F	A377T	2	4.6	ND	122	325	81	**111**	8.7	**1.0**	**4.1**	0.8
F3-I1	F	ND	54	5.2	1.2	131	347	88	280	**9.3**	3.2	1.5	0.3
F3-I2	M	Y401N	56	5.0	2.0	160	**360**	86	**125**	**9.8**	4.4	2.3	0.5
F3-II1	F	ND	29	4.8	1.1	130	347	**79**	285	**10.4**	7.5	**5.0**	0.6
F3-II2	M	Y401N	21	4.7	1.3	147	350	88	**112**	**10.0**	2.1	1.8	0.3
F3-II3	F	ND	22	4.9	0.5	139	**352**	80	389	**9.6**	3.1	1.6	0.4
F3-II4	F	Y401N	16	4.4	1.3	145	350	87	**80**	**9.4**	2.5	1.5	0.3

F4-I1	F	WT	55	**3.9**	ND	120	348	88	209	9	3.1	**4.9**	0.2
F4-I2	M	I358M	56	4.6	ND	149	**353**	91	**57**	**11.7**	2.6	1.6	0.5
F4-II1*	M	I358M	24	**3.0**	ND	125	349	92	**29**	**10.7**	**1.5**	2.1	0.5
F4-II2	F	I358M	30	4.3	ND	142	**351**	95	**134**	**10.5**	2.5	1.5	0.7
F4-II3	F	I358M	27	4.1	ND	142	**351**	98	**121**	**9.8**	2.8	1.9	0.7
F5-I2	M	R396G	59	ND	ND	140	ND	ND	**58**	**10.8**	ND	3.5	ND
F5-II1	F	R396G	26	ND	ND	133	ND	ND	**76**	**11.2**	ND	4.0	ND
F5-II2	F	R396G	20	ND	ND	109	ND	ND	**75**	**9.9**	ND	3.9	ND
F6-I1	F	WT	ND	4.4	ND	137	ND	ND	199	ND	ND	ND	ND
F6-II1	F	Y401H	ND	**3.9**	ND	132	ND	**100**	**77**	ND	ND	ND	ND
F6-II2	F	ND	ND	ND	ND	ND	ND	ND	159	ND	ND	ND	ND

*in remission (2 year after chemotherapy)

ND not done

Bold values are outside the normal range

Figure legends

Figure 1: Identification of variants in *ETV6* underlying AD thrombocytopenia, megakaryocyte and platelet characteristics

(a) Schematic representation of the different domains of the ETV6 protein. The N-terminal domain (PNT), central domain and C-terminal domain containing a DNA-binding domain (ETS) are depicted. Arrows indicate the location of the ETV6 variants and the corresponding family is mentioned into brackets.

(b) Pedigrees for the affected families. Squares denote males, circles denote females and slashes represent deceased family members. Black filled symbols represent thrombocytopenic family members and dotted line symbols represent non-tested members. The families F1, F2, F3, F4, F5 and F6 carried the ETV6 p.P214L, p.A377T, p.Y401N, p.I358M, p.R396G and p.Y401H variants, respectively, which segregated with thrombocytopenia. See Table for blood cell count values.

(c) Sex-stratified histograms of platelet count and mean platelet volume measurements obtained using a Coulter haematology analyser from 480,001 UK Biobank volunteers after adjustment for technical artefacts. The red arrows superimposed upon the histograms indicate the sex and values for patients with a deleterious variant in ETV6. The green arrows indicate the sex and values for relatives homozygous for the corresponding wildtype allele.

(d) BM smears (May-Grünwald Giemsa staining) from family F1 propositus (F1-IV3). Left: a relatively immature MK with reduced cytoplasm. Middle: a micromegakaryocyte without granules, with immature cytoplasm (basophilic) and nucleus. Signs of impaired proplatelet formation can be observed. Right: a mature megakaryocyte of reduced size with a hypolobulated nucleus. Table indicates the % of megakaryocytes at each stage of maturation in the BM samples from family F1 proposita (F1-IVI3) and a healthy control.

(e) Ultrastructural aspects of platelets from patients F3-I2 and F3-II4, F4-I2 and F4-II3 and unrelated healthy controls. Upper panel: aspect of healthy platelets; middle panel: serie of mostly rounder platelets from patients F4-I2 and F4-II3, lower panel: a serie of platelets emphasizing anisocytosis in F3-II4 patient and a platelet from patient F3-I2 with abnormal membrane complex (MC). Note the heterogeneous presence of α-granules with an occasional granule of increased size.

(f) The platelet area and roundness was quantified. Perfect round platelets would have a value of 1. Values are the means and SD as quantified for 50 randomly selected platelets per subject using two-tailed unpaired t-test with Welch's correction. *** $p<0.0001$.

Figure 2: Effect of the variants on repressive activity and co-repressor recruitment.

(a) Western blot analysis of ETV6 expression in platelets of 6 affected F1 members and 7 external controls. GAPDH was used as a protein loading control.

(b-c) GripTite™ 293 MSR cells were co-transfected with the luciferase reporter plasmid containing 3 tandem copies of the Ets Binding Site (EBS) upstream of HSV-Tk (E743tk80Luc), pCDNA3.1 expression vector (empty, wt or mutETV6) or pGL473 Renilla luciferase control vector. **(b)** Western blot analysis of ETV6 expression in whole cell lysates of GripTite™ 293 MSR transfected with wtETV6 or mutETV6 expression vectors. GAPDH was used as a protein loading control. The data are representative of 4 to 8 independent experiments. **(c)** The firefly to renilla luminescence ratios (Fluc/Rluc) were calculated to compensate for transfection efficiency. The data represent the mean ± SEM of 4 to 8 independent experiments, student's t-test *** $p< 0.001$ (each condition was compared with wt).

(d) Effects of the ETV6 variants on co-repressor recruitment. Mammalian two-hybrid analysis of the protein interactions between wt N-CoR, SMRT or mSin3A (expressed using the GAL4(DBD) plasmid) and wtETV6 or mutETV6 (expressed using the GAL4-VP16 activation domain vector). The results are expressed as mean ± SEM of 3 to 8 independent experiments, student's t-test *$p<0.05$, **$p< 0.01$, *** $p< 0.001$.

(e) Immunoprecipitation of endogenous co-repressor SMRT and ETV6 from GripTite™ 293 MSR cells transfected with wt and mutETV6. Immunoprecipitation was performed on cell lysates with ETV6 antibody. The total cell lysates (lower panel) and immunoprecipitates (upper panel) were analyzed via immunoblotting with anti-SMRT antibody. Quantification of band intensity for SMRT and SMRT-extended (SMRTe) is shown below the western blot. The results are expressed as mean ± SEM, student's t-test, *$p<0.05$ vs. wt.

Figure 3: Increased numbers of circulating CD34 positive cells in variant carriers.

Flow cytometry analysis of $CD34^+$ cells. **(a)** Representative $CD34^+/CD38^+$ dot plot of cells from 2 controls and 1 patient (F1-III7). **(b)** Histograms show the percentage of $CD34^+$ cells in 8 controls and 5 affected family members (F1-III3, F1-III7, F1-III8, F1-IV1, F1-IV3) (mean ± SEM, student's t-test, **$p<0.01$).

Figure 4: Megakaryocyte differentiation and colony-forming cell potential.

(a-c) *In vitro* MK differentiation in control or patient peripheral blood $CD34^+$ cells, the cells were analyzed at culture day 10. **(a)** The data show a representative dot plot of CD41 and CD42a expression in $Hoechst^+$ cells from a control individual and F1-III6. The gate represents mature MKs. **(b)** The histogram represents the MK ($CD41^+CD42a^+Hoechst^+$) numbers (nb) in the affected family members (n=9) expressed as fold increase over healthy controls (n=10), student's t-test, **$p< 0.01$. **(c)** The ploidy level (N) was analyzed for $CD41^+CD42a^+$ MKs, and mean ploidy was calculated using the percentage of cells with 2N, 4N, 8N, 16N and 32N.

(d) Methylcellulose assay. The histograms present the number of erythroid (BFU-E), granulo-monocyte (CFU-G/M/GM) and mixed (CFU-GEMM) progenitors from two patients of family F3 with the

p.Y401N variant (F3-I2 and F3-II4) and two independent controls. Mean ± SEM, student's t-test, *p<0.05.

(e) Fibrin clot culture. The histograms present the number of MK progenitors (CFU-MK) from two independent controls and two patients (F3-I2 and F3-II4). The CFU-MKs are divided in four categories: <5 MKs per colony, 5-10 MKs per colony, 10-50 MKs per colony or >50 MKs per colony. Error bars represent ± SD of triplicate experiments.

(f) Representative pictures of CFU-MKs after CD41 immunostaining. Control 1 and Control 2 represent 2 independent controls, and F3-I2 and F3-II4 are two affected patients.

Figure 5: *ETV6* variants lead to defective proplatelet (PPT) formation.

(a-b) *In vitro* MK differentiation induced from control or patient peripheral blood $CD34^+$ progenitors in the presence of TPO and SCF. **(a)** Representative microscopic images of PPT formation in control (n=2) and patient (F1-III7, F1-III3) MKs after 11 or 13 days of culture. **(b)** The histograms show the percentage of PPT-bearing MKs from members of 2 families (F1-III3, F1-IV3, F1-III7, F3-I2, F3-II4) and 5 independent controls evaluated (3 to 5 evaluations) between culture days 10 to 15. The percentage of PPT-forming MKs was estimated by counting MKs exhibiting ≥1 cytoplasmic processes with areas of constriction. Double-blinded researchers quantified a total of 300-500 cells. The results are expressed as mean ± SEM, student's t-test **p<0.01 and ***p<0.001. **(c)** F-actin and β-tubulin staining on PPT-forming MKs from F1-III3 and a control individual, adhering to fibrinogen. Confocal images were acquired at day 12 of culture (x60). **(d)** *In vitro* MK differentiation was induced from control peripheral blood $CD34^+$ progenitors transduced with wt or mutETV6 (family F1, c.641C>T, p.P214L) lentiviral particles in the presence of TPO and SCF. Microscopic images of PPT formation were acquired at days 13 and 15 of culture.

Figure 6: Rho-GTPase expression analysis.

(a) Western blot analysis and quantification of Cdc42**,** Rac1 and RhoA expression in platelet lysates from healthy controls (n=7 for Cdc42, n=4 for Rac1, n=4 for RhoA) and affected members from F1 (n=6 for Cdc42, n=4 for Rac1 and n=5 for RhoA). GAPDH was used as a protein loading control. The results are expressed as mean ± SEM, student's t-test *p<0.05 and ***p<0.001.

(b) Quantification of Cdc42, Rac1 and RhoA mRNA levels in $CD34^+$-derived MKs from healthy controls (n=10) and affected family members from F1 (n=6) and F3 (n=2). mRNA expression levels were measured via RT-PCR, and expression levels were normalized to housekeeping 36b4 RNA. The results are expressed as mean ± SEM, student's t-test, **p<0.005.

(c) Western blot analysis and quantification of Cdc42, RhoA and GAPDH expression in platelets from two affected members of the F3 family (F3-I2 and F3-II4) and a healthy control.

(d) *In vitro* MK differentiation was induced from F1-III7 $CD34^+$ progenitors transduced with control or Cdc42 lentiviral particles in the presence of TPO and SCF. Microscopic images of PPT formation were

acquired at days 14 and 16 of culture. The arrows indicate thinner proplatelet extensions and swellings in the presence of Cdc42. Extensions were enlarged in the control.

Figure 7: Platelet spreading and clot retraction.

(a) Left: Representative images of unstimulated platelets spread over immobilized fibronectin. Middle: filopodia formation was quantified according to the number of extensions per unstimulated platelet derived from affected individuals (F1-III3, F1-III7) and healthy controls (n=2). Right: Quantification of lamellipodia-forming cells, at resting and ADP-stimulated conditions, from affected members (F1-III7, F1-III8) and healthy controls (n=2). The data are expressed as mean ± SEM of 5 different view fields. Student's t-test, ***p<0.001.

(b) Actin polymerization quantification in spread unstimulated platelets. Left: representative images of G-actin, F-actin and the G-actin/F-actin ratio in control platelets and the rare spread platelets detected in F1-III7. Platelets were spread over fibronectin and stimulated with ADP. Right: quantification of the area with the high G-actin/F-actin ratio. Quantification of the ratio was performed according to the lookup table as the percentage of the platelet surface (n=20 different cells; mean ± SEM. Student's t-test *p<0.05).

(c) Clot retraction. Left: representative images at 0, 30 and 50 minutes. Right: quantification of the extent of clot retraction expressed as percentage the initial clot (mean ± SEM, n=2 for F1-III7 and n=4 for controls. Two-way ANOVA, ***p<0.001).

Figure 1

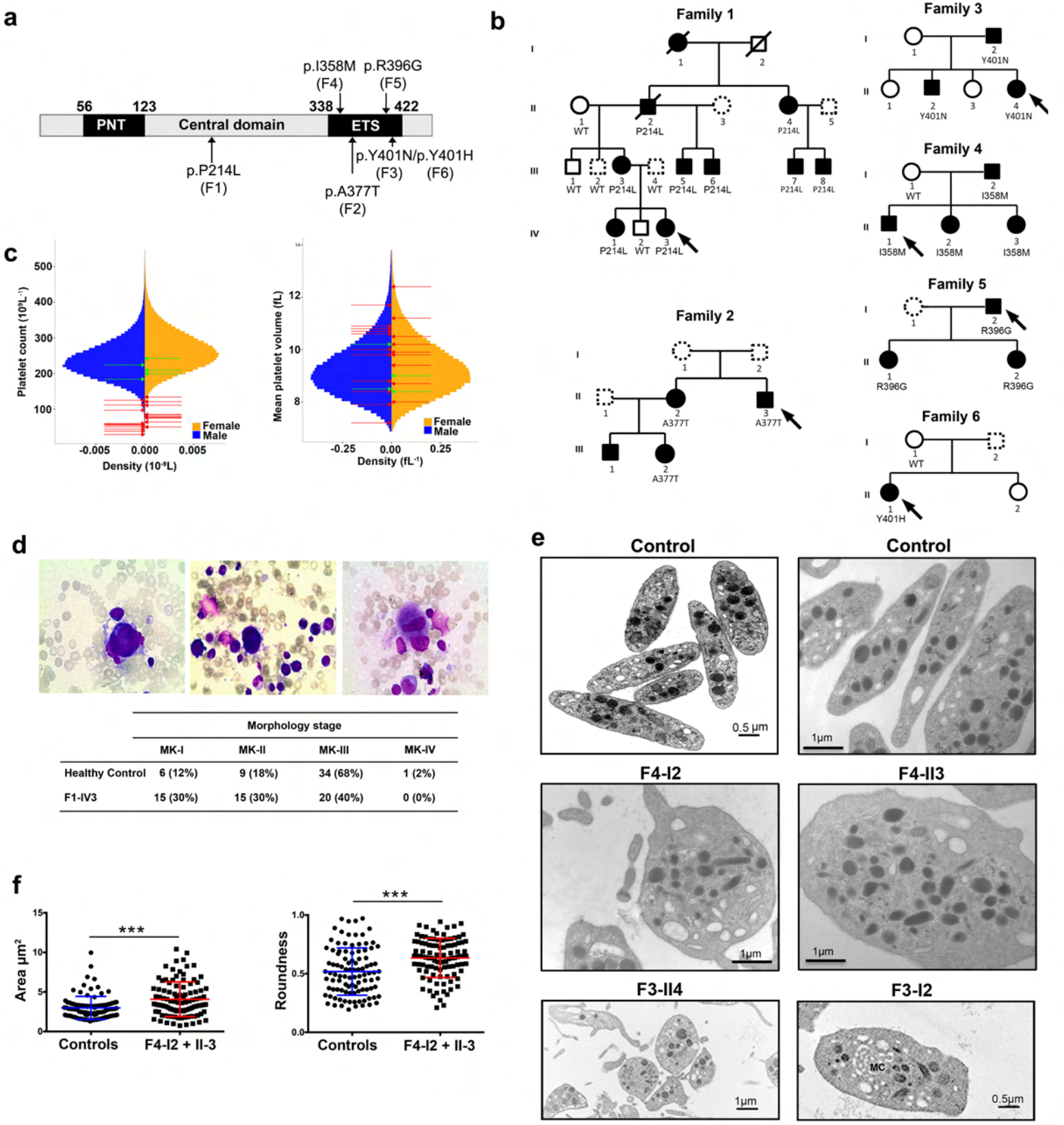

	Morphology stage			
	MK-I	MK-II	MK-III	MK-IV
Healthy Control	6 (12%)	9 (18%)	34 (68%)	1 (2%)
F1-IV3	15 (30%)	15 (30%)	20 (40%)	0 (0%)

Figure 2

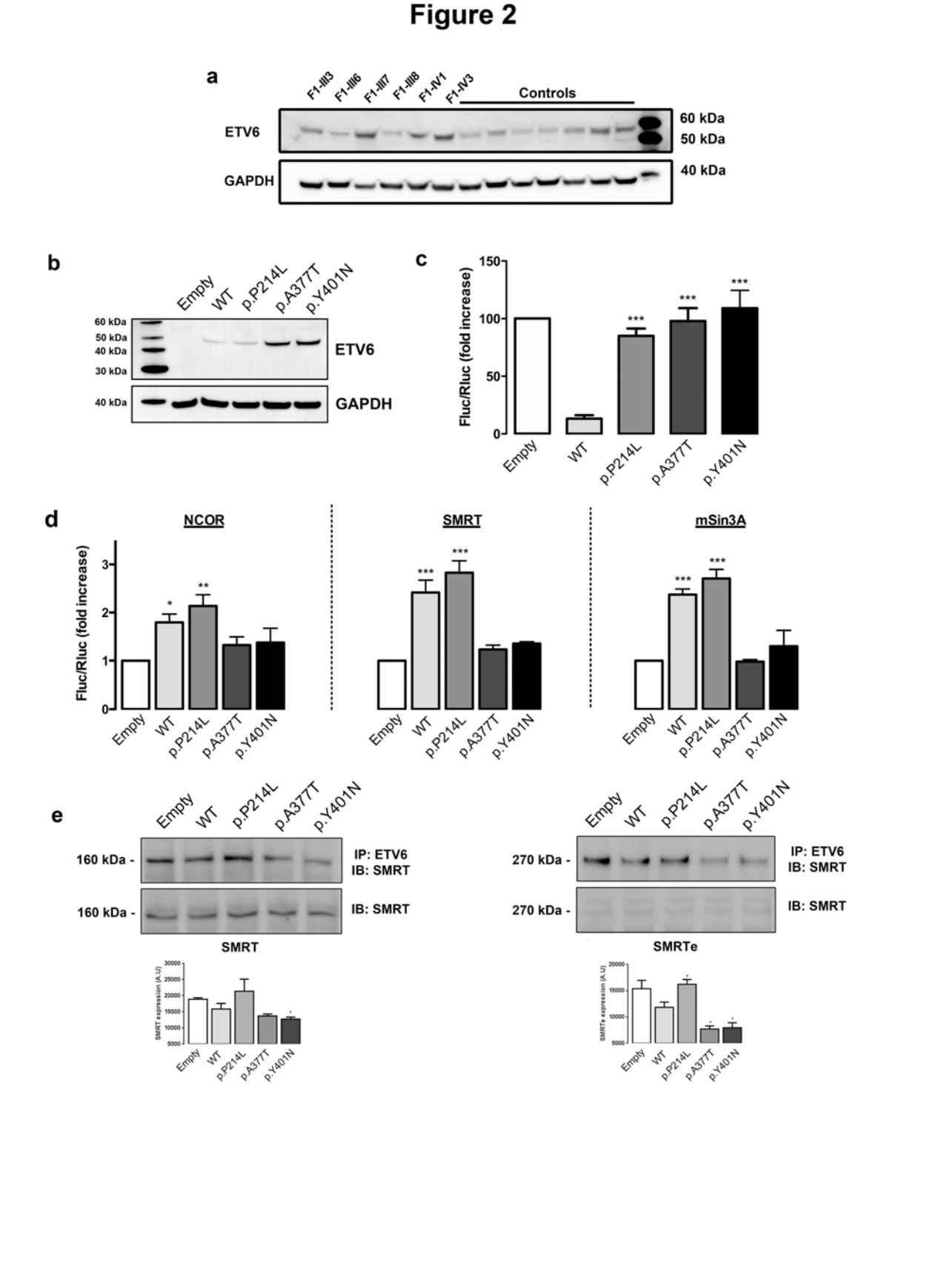
a
F1-III3
F1-III6
F1-III7
F1-III8
F1-IV1
F1-IV3
Controls
ETV6
GAPDH
60 kDa
50 kDa
40 kDa
b
Empty
WT
p.P214L
p.A377T
p.Y401N
60 kDa
50 kDa
40 kDa
30 kDa
ETV6
40 kDa
GAPDH
c
Fluc/Rluc (fold increase)
150
100
50
0
***
Empty
WT
p.P214L
p.A377T
p.Y401N
d
NCOR
SMRT
mSin3A
Fluc/Rluc (fold increase)
3
2
1
0
*
**
***
Empty
WT
p.P214L
p.A377T
p.Y401N
e
Empty
WT
p.P214L
p.A377T
p.Y401N
160 kDa -
IP: ETV6
IB: SMRT
IB: SMRT
SMRT
SMRT expression (A.U)
270 kDa -
SMRTe
SMRTe expression (A.U)

Figure 3

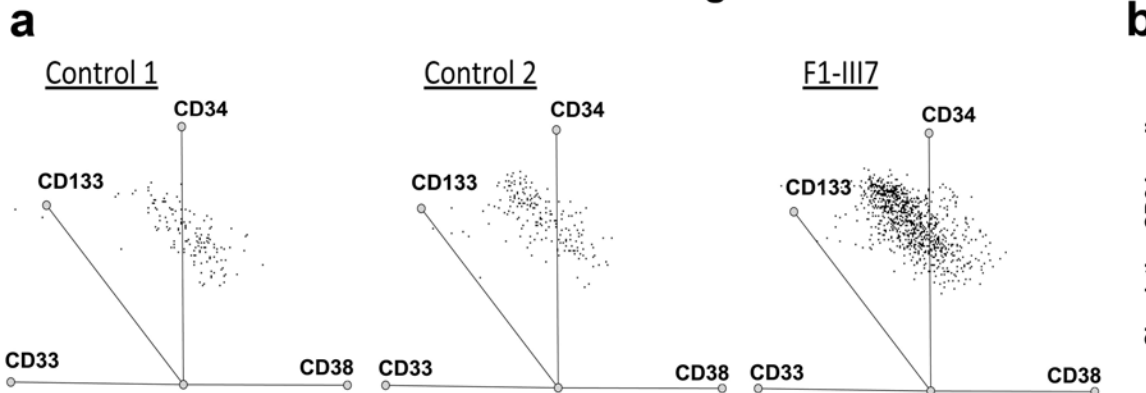
a
Control 1
CD34
CD133
CD33
CD38
Control 2
CD34
CD133
CD33
CD38
F1-III7
CD34
CD133
CD33
CD38
b
Circulating CD34+ cells
(% of leukocytes)
0.20
0.15
0.10
0.05
0.00
**
Controls
Affected members

Figure 4

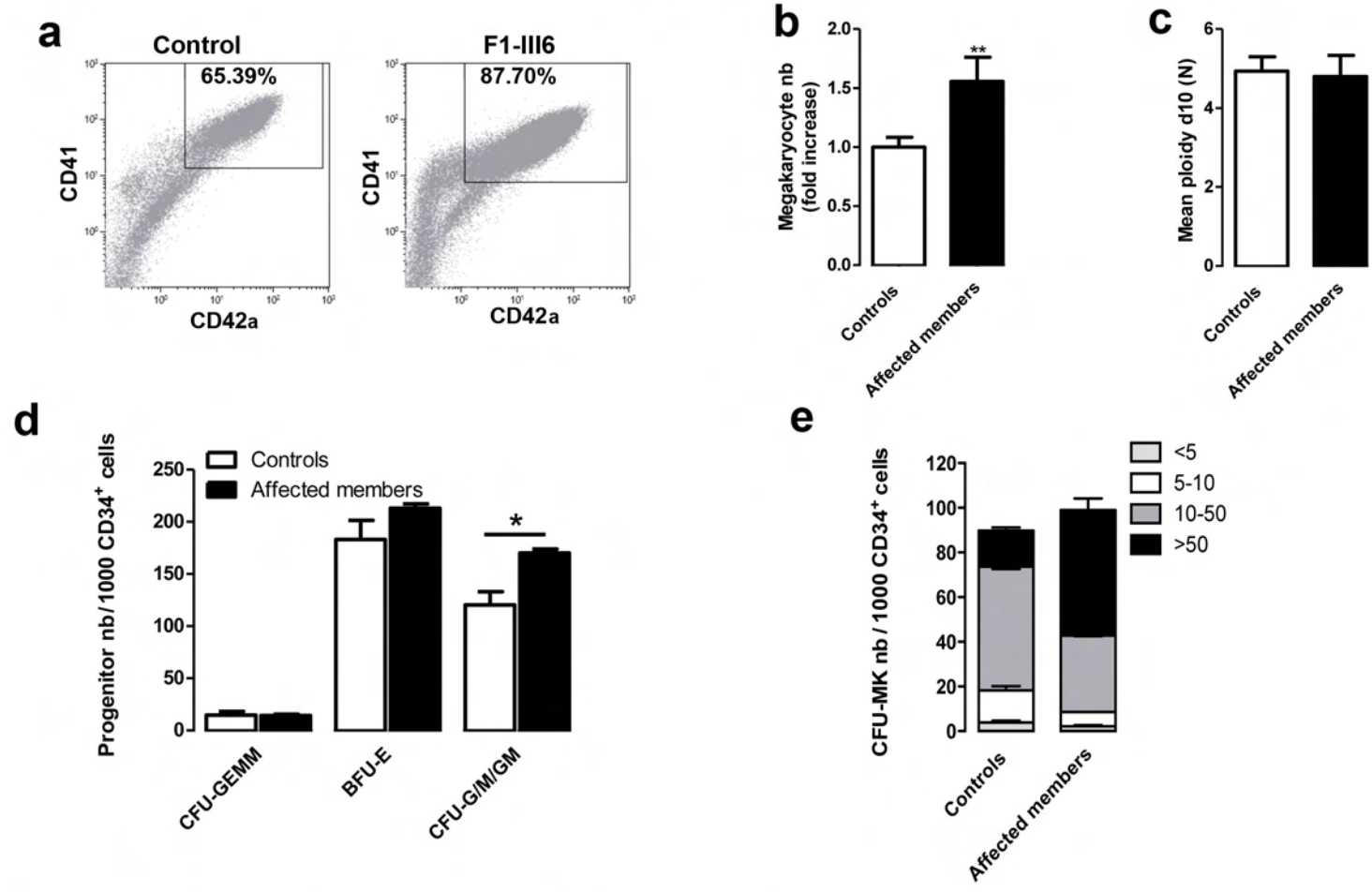
a
Control
65.39%
F1-III6
87.70%
CD41
CD42a
b
Megakaryocyte nb (fold increase)
**
Controls
Affected members
c
Mean ploidy d10 (N)
Controls
Affected members
d
Progenitor nb/1000 CD34+ cells
Controls
Affected members
*
CFU-GEMM
BFU-E
CFU-G/M/GM
e
CFU-MK nb / 1000 CD34+ cells
<5
5-10
10-50
>50
Controls
Affected members
f
Control 1
Control 2
F3-I2
F3-II4
200 µm

Figure 5

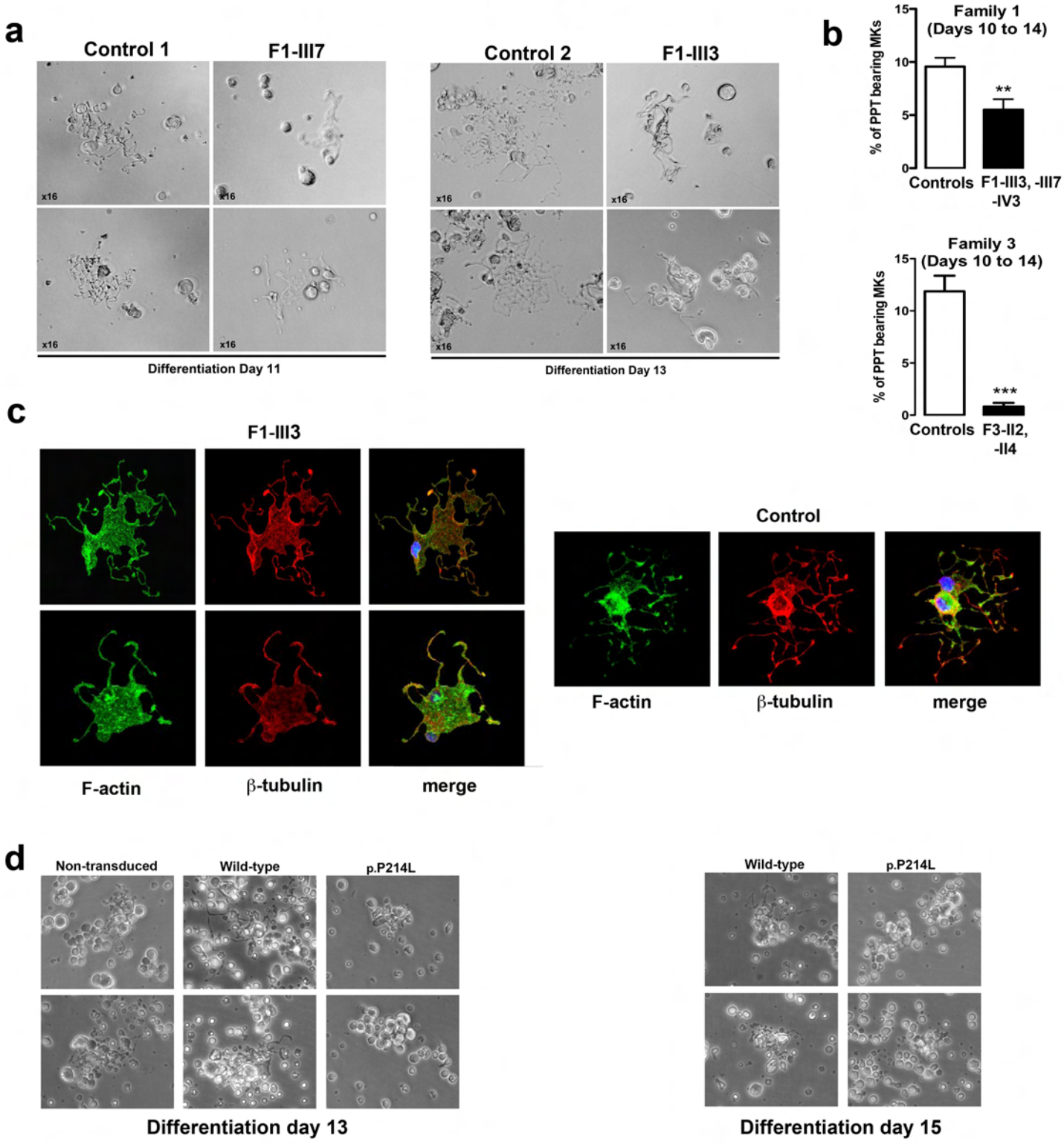
a
Control 1
F1-III7
Control 2
F1-III3
x16
Differentiation Day 11
Differentiation Day 13
b
Family 1
(Days 10 to 14)
% of PPT bearing MKs
15
10
5
0
**
Controls
F1-III3, -III7
-IV3
Family 3
(Days 10 to 14)
% of PPT bearing MKs
***
Controls
F3-II2,
-II4
c
F1-III3
F-actin
β-tubulin
merge
Control
F-actin
β-tubulin
merge
d
Non-transduced
Wild-type
p.P214L
Differentiation day 13
Wild-type
p.P214L
Differentiation day 15

Figure 6

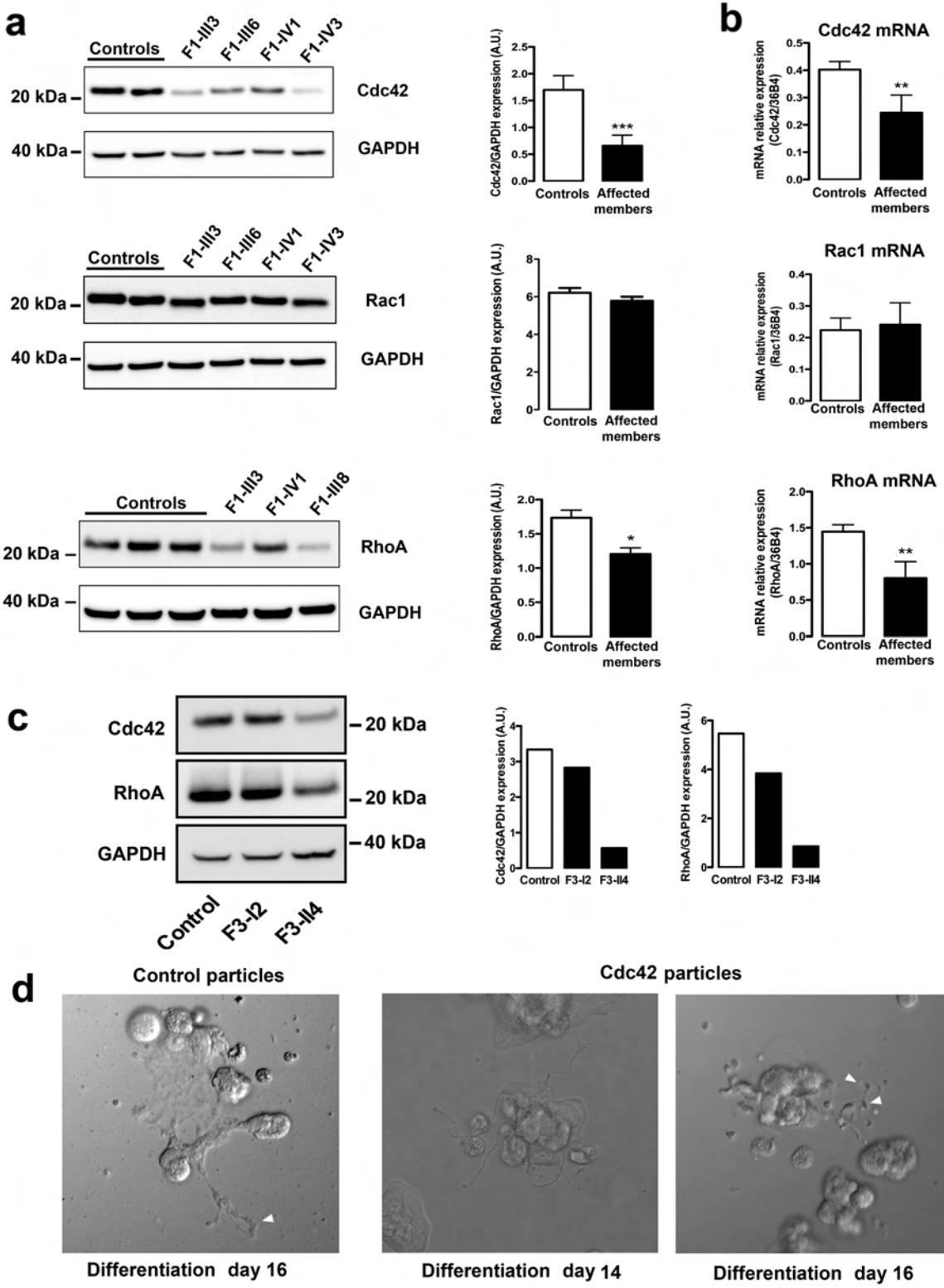
a
Controls
F1-III3
F1-III6
F1-IV1
F1-IV3
20 kDa
Cdc42
40 kDa
GAPDH
Cdc42/GAPDH expression (A.U.)
Controls
Affected members
b
Cdc42 mRNA
mRNA relative expression (Cdc42/36B4)
Rac1
Rac1/GAPDH expression (A.U.)
Rac1 mRNA
mRNA relative expression (Rac1/36B4)
F1-III8
RhoA
RhoA/GAPDH expression (A.U.)
RhoA mRNA
mRNA relative expression (RhoA/36B4)
c
Control
F3-I2
F3-II4
d
Control particles
Cdc42 particles
Differentiation day 16
Differentiation day 14
Differentiation day 16

Figure 7

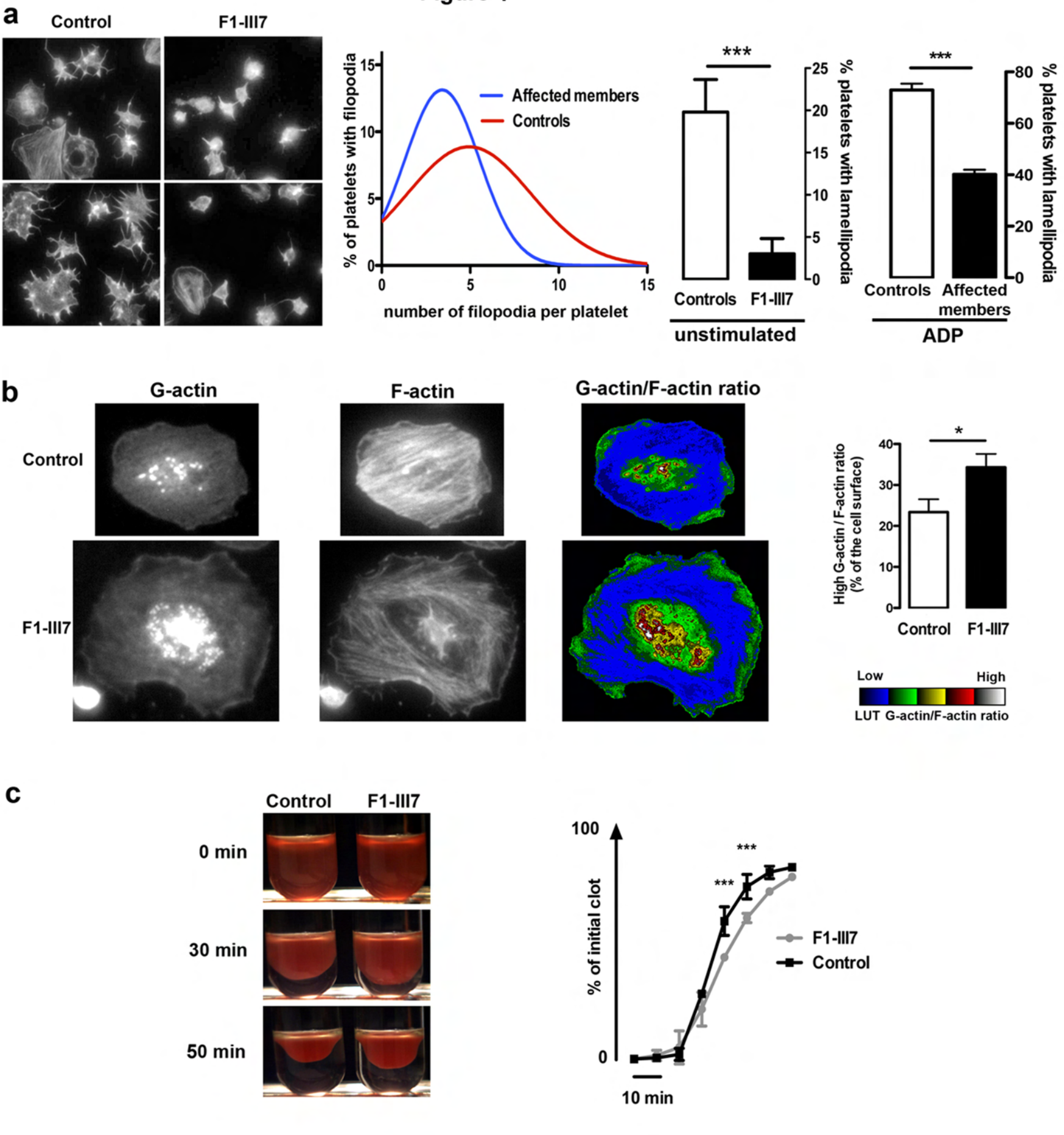
a
Control
F1-III7
% of platelets with filopodia
number of filopodia per platelet
Affected members
Controls
***
% platelets with lamellipodia
Controls
F1-III7
unstimulated
Controls
Affected members
ADP
b
G-actin
F-actin
G-actin/F-actin ratio
Control
F1-III7
High G-actin / F-actin ratio (% of the cell surface)
*
Low
High
LUT G-actin/F-actin ratio
c
Control
F1-III7
0 min
30 min
50 min
% of initial clot
100
0
10 min
F1-III7
Control

Supplemental methods

Exome sequencing and sequencing validation in the F1 family

Whole-exome sequencing was performed on genomic DNA, as previously described[1], from 6 members of F1: the index case (F1-IV3), 2 unaffected members (F1-II1 and F1-IV2) and 3 affected members (F1-II2, F1-III3 and F1-III8). Direct Sanger sequencing confirmed the genotype among all family members (Big Dye Terminator kit V3; Life Technologies). Sequences were subsequently analyzed (Chromas X software) and aligned (Multalign: http://multalin.toulouse.inra.fr/multalin/).

Antibodies

Immunoblots were performed using goat polyclonal anti-ETV6 (N19, #sc8546, Santa Cruz), mouse monoclonal anti-SMRT (1212, #sc32298, Santa Cruz), rabbit polyclonal anti-RhoA (119, #sc179, Santa Cruz), rabbit polyclonal anti-MYH10 (#3404, Cell Signaling Technology), mouse monoclonal anti-Cdc42 (#05-542, Millipore), mouse monoclonal anti-Rac1 (23A8, #05-389, Millipore) and mouse monoclonal anti-GAPDH (6C5, MAB374, Millipore) antibodies.

Real-Time PCR

cDNA was synthesized using MMLV-reverse transcriptase from 10 ng of total RNA. Real-time PCR were performed using a LightCycler 480 (Roche) and Eva Green MasterMix (Euromedex). Relative levels of mRNA were measured using the comparative CT method. Primer sequences are available upon request.

Quantification of circulating $CD34^+$ hematopoietic progenitors in the blood

Before labeling, 2 mL of each blood sample was subjected to red blood cell lysis. Equivalent numbers of cells were incubated for 15 minutes at 20°C with the appropriate monoclonal antibody cocktails: CD133-PhycoErythrin (BD Biosciences), CD19-FITC, CD34-AlloPhyco Cyanin/Alexa Fluor750, CD3-Pacific Blue, CD45-Krome Orange, CD33-PE/Cyanin7, CD38-AlloPhyco Cyanin, CD41-PE/Cyanin5, CD42b-PE/Cyanin5, CD61-FITC and CD123-PE (Beckman Coulter). Progenitors were characterized by CD34/CD133/CD33/CD38 co-expression; cells were gated on the $CD34^+$ and $SS^{low}/CD45^{low}$ population and excluded co-expression of lymphoid markers (Navios, Beckman Coulter).

Glycoprotein surface expression on platelets

PRPs were incubated in the presence or absence of platelet agonist ADP (10 µM) or TRAP (50 µM) with antibodies against $\alpha_{IIb}\beta_3$ (clone P2), the active form of $\alpha_{IIb}\beta_3$ (clone PAC-1; BD), glycoprotein (GP) Ibα, Ia, IV, CD63 (clone CLB-grad12; Beckman Coulter) and CD62P (clone CLB-Thromb/6) for 30 min at 20°C. Scatter signals and fluorescence intensity were analyzed using a FC500 flow cytometer (Beckman Coulter**).**

Platelet survival assay

The platelet survival assay was based on the method of Thakur *et al.*[2]. Autologous platelets were washed and incubated with 3 MBq of ^{111}In-oxine for 10 min at 37° C. The platelets were then washed

and suspended in autologous platelet-poor plasma. An aliquot was withdrawn for platelet count and measurement of labeling efficiency. The remainder of the labeled platelets was used for intravenous administration. Successive blood samples were collected at 15 minutes as well as 2, 24, 48, 72, 96, 120 and 144 hours post-injection for platelet count and radioactivity quantification. An exponential model was used to calculate platelet survival time according to the International Committee for Standardization in Hematology (ICSH).[3] The platelet recovery and platelet production rates were calculated based on platelet survival time, initial platelet recovery and platelet count.

Platelet spreading analysis

Non-stimulated or ADP-stimulated (10 µM) washed platelets (10^7 platelets/ml) were allowed to adhere (45 min, 37°C) to fibronectin-coated coverslips (20 µg/ml; Sigma-Aldrich). Fixed platelets were stained with Alexa 488-phalloidin (F-actin) and Alexa 594-DNAse I (G-actin). Images were recorded (Axio-Imager M1 microscope with an Axiocam MRm camera; Carl Zeiss) and analyzed (ImageJ software). Filopodia and lamellipodia were manually quantified in five different view fields. The G-actin/F-actin ratio was evaluated on 20 different platelets. For each pixel, the G-actin fluorescence intensity was divided by the corresponding F-actin signal. A 5-ramps look-up table was applied to the ratio image. The surface of high G-actin/F-actin ratio corresponded to the platelet area with a signal above the LUT threshold, defined as $\geq$3. Measurements were made on unprocessed images obtained using the same staining conditions, microscope objective and settings, and camera exposure time.

Clot retraction

PRPs were diluted in Tyrode's buffer with red blood cells. Coagulation was triggered using thrombin (1.25 U/mL), and clots were allowed to retract (1h, 37°C). Images were recorded using a CoolSNAP CCD-camera and analyzed to evaluate the reduction (%) of the initial clot surface (ImageJ software).

Co-immunoprecipitation assay

Whole cell extracts were prepared in 20 mM Tris, 140 mM NaCl, 1 mM EDTA and 0.05% Nonidet P-40, with EDTA-free protease cocktail inhibitor. The cell lysates were pre-cleared with protein A/G magnetic beads (Millipore) for 2 hours at 4ºC. The immunoprecipitation was carried out overnight at 4^oC via incubation of cell extracts (500 µg protein) with anti-ETV6-coated beads. Immunoprecipitates were washed five times with lysis buffer, suspended in SDS sample buffer and boiled for 5 min at 95 ºC. The bound proteins were assessed for SMRT expression (Santa Cruz) via western blotting.

Cell transfection and luciferase assays

Transcriptional regulatory properties of wt*ETV6* and mut*ETV6* were analyzed using $p(E74)_3$tk80Luc plasmid containing the luciferase gene driven by an enhancer/promoter cassette composed of three tandem copies of the Ets Binding Site (E74-binding sites AACCGGAAGTA, found in the Drosophila E74 gene promoter) inserted 5′ of the herpes simplex virus thymidine kinase promoter. This plasmid was a gift from J Ghysdael[4]. GripTite™ 293 MSR Cells were transfected with the indicated reporter gene constructs (166 ng), the expression plasmid (333 ng) and pGL473-hRLuc

(50 ng) to normalize transfection efficiency. Luciferase activity was assayed 48 hours after transfection (Dual-Luciferase® Reporter Assay system, Promega).

Mammalian two-hybrid experiments. GripTite™ 293 MSR cells were co-transfected with GAL4$(UAS)_5$-TkLUC reporter plasmid (166 ng); GAL4(DBD)-N-CoR, GAL4(DBD)-SMRT, or GAL4(DBD)-mSin3A expression vector (or an empty vector, pGALO) (166 ng); expression vector pVP16-wtETV6 or pVP16-mutETV6 (166 ng) and pGL4-hRLuc (50 ng) to normalize transfection efficiency[5]. Luciferase activity was assayed 48 hours after transfection.

Ploidy analysis

At culture day 10, Hoechst 33342 (10 µg/mL; Sigma-Aldrich) was added to the medium of cultured MKs for 1 hour at 37°C. The cells were then stained with directly coupled monoclonal antibodies: anti–CD41-allophycocyanin and anti-CD42a-phycoerythrin (BD Pharmingen) for 10 minutes at 4°C. Ploidy was measured on the $CD41^+CD42^+$ cell population by means of a flow cytometer (Navios BD Biosciences) and calculated as previously described.[6]

Quantification of proplatelet-bearing MKs

PPT-forming MKs were quantified on 300-500 total cells between days 11 and 15 of culture. PPT-bearing MKs exhibited cytoplasmic extensions with constriction areas (3 separate culture wells for each individual and condition). Microtubule and F-actin organization was determined on MKs (12 days) adhering to fibrinogen with fluorescently labeled anti-tubulin antibody (Sigma-Aldrich) and phalloidin (Life Technologies).

Lentiviral particle production and CD34+ cell transduction

Wild-type (wt) and p.P214L ETV6 DNA were subcloned into a third generation of HIV-derived lentiviral vector pRRLsin-PGK-IRES2-eGFP-WPRE (Genethon), and lentiviral stocks were prepared as previously described.[7, 8] CDC42 DNA was subcloned into pRRLsin-PGK-IRES-ZsGreenGFP-WPRE, and lentiviral particles were produced by Vect'UB (Plateforme de Vectorologie, Bordeaux, France). $CD34^+$ cells (3.5 to $5x10^4$) were infected twice with lentiviral particles. After 8 hours, the cells were washed and cultured in serum-free medium supplemented with TPO (100 ng/ml) and SCF (250 ng/ml).

Supplemental figure 1

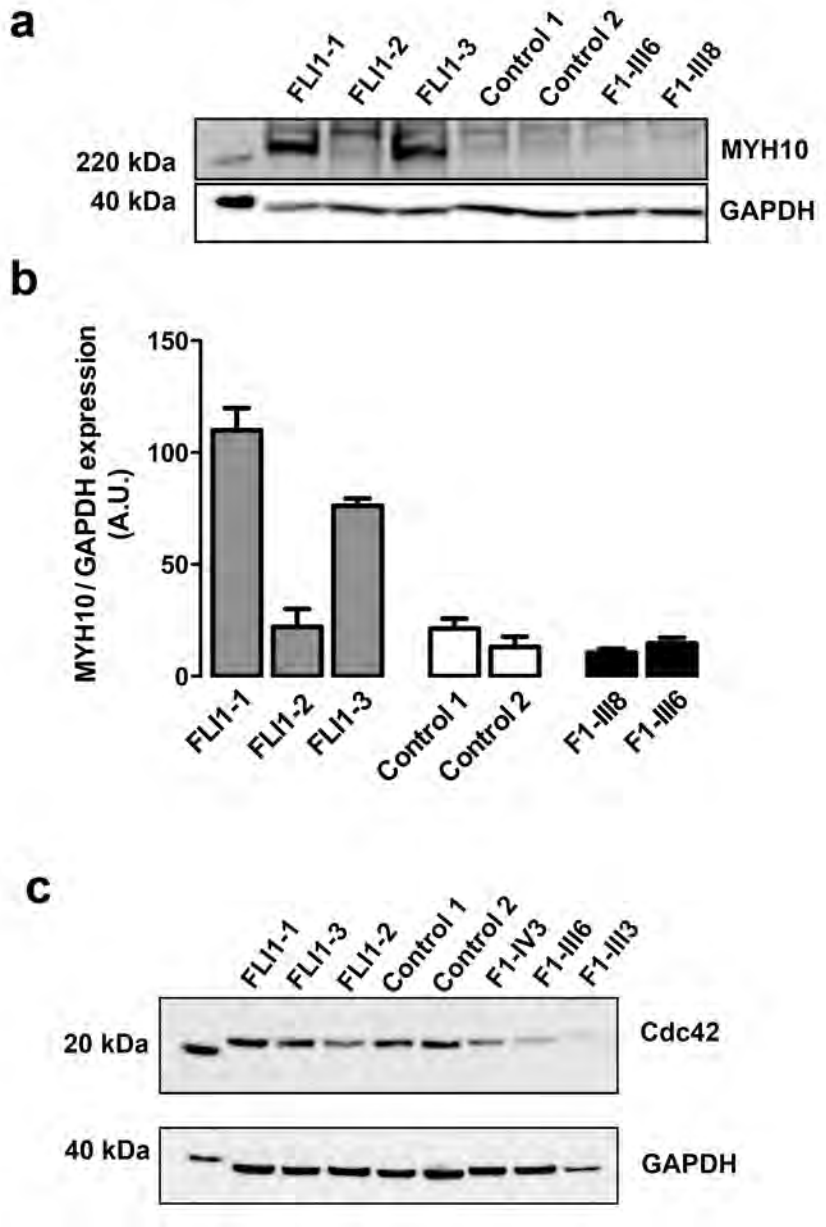

Supplementary Figure 1: Effect of ETV6 mutations on MYH10 levels.

Western blot analysis **(a)** and quantification of MYH10 **(b)** and Cdc42 (**c**) expression in platelets of affected members (F1-III3, F1-III6, F1-III8, F1-IV3), 2 healthy controls and members of family affected by a FLI1 mutation: 2 carriers of the mutation (FLI1-1, FLI1-3) and 1 non-carrier (FLI1-2). GAPDH was used as a protein loading control. First lane corresponds to the protein ladder. The results are expressed as mean ± SEM, n=2.

Supplemental Table 1: Summarized results of platelet aggregation, ATP secretion and dense granule defects by electron microscopy or a mepacrine uptake assay. Human Phenotype Ontology (HPO) phenotyping was used as described (PMID: 25949529) to present the functional platelet laboratory results. As the different laboratories have used different type of aggregometers, concentrations of agonists and dense granule studies, the HPO methodology allows standard platelet function phenotyping of laboratory data. As expected, platelet aggregation performed with platelet rich plasma containing < 120 x 10^3 platelets/µL plasma is highly variable and was not included in the analysis.

	Impaired ADP-induced platelet aggregation	Impaired epinephrine-induced platelet aggregation	Impaired collagen-induced platelet aggregation	Impaired arachidonic acid-induced platelet aggregation	Impaired ristocetin-induced platelet aggregation	Impaired thrombin-induced platelet aggregation	Impaired thromboxan A2 analog-induced platelet aggregation	Abnormal platelet ATP dense granule secretion	Abnormal dense granule
F1-III3	Yes	No	No	Yes	Yes	*ND*	*ND*	*ND*	No
F2-II3	No	No	No	Yes	No	No	No	No	No
F3-II4	No	No	No	Yes	No	No	Yes	No	No
F4-I2	No	Yes	No	Yes	No	No	No	No	No
F4-II2	No	Yes	No	Yes	*ND*	No	No	No	No
F4-II3	No	Yes	No	Yes	*ND*	No	No	No	No
F5-I2	No	No	No	Yes	No	*ND*	No	No	No
F5-II1	No	No	No	No	No	*ND*	*ND*	No	No
F6-I1 (WT)	No	No	No	No	*ND*	No	No	Yes	Yes
F6-II1	Yes	Yes	Yes	Yes	*ND*	*ND*	No	No	Yes

ND: not done

Supplemental Table 2: Flow Cytometric Analysis of Platelet-Membrane Glycoproteins

Baseline	αIIbβ3 (P2)	αIIbβ3 (Pac1)	GPIb	GPIa	GPIV	CD63	CD62P
MFI Normal range	23-40	2.8-6.9	21-40	1.8-6.9	6.0-16	0.3-0.9	1.1-4.3
F1-II2	29	2.1	23	2.2	5.9	0.2	2.0
F1-III3	37	3.3	35	3.4	5.4	1.6	1.9
F1-III5	30	2.9	18	3.0	5.1	0.4	2.2
F1-IV3	22	2.3	21	2.8	7.0	0.6	2.9

ADP (10 μM)	αIIbβ3 (P2)	αIIbβ3 (Pac1)	GPIb	GPIa	GPIV	GP53	CD62P
MFI Normal range	23-45	5.4-16	5-21	2.2-6.7	6.7-19	0.4-1.2	3.2-16
F1-II2	32	3.1	9.8	ND	ND	0.3	3.2
F1-III3	45	20	16	ND	ND	2.1	8.5
F1-III5	22	17	4.8	ND	ND	0.6	6.8
F1-IV3	24	12	8.3	ND	ND	0.7	7.9

TRAP (50 μM)	αIIbβ3 (P2)	αIIbβ3 (Pac1)	GPIb	GPIa	GPIV	GP53	CD62P
MFI Normal range	29-55	3.5-9	10-27	2.0-6.5	7.2-18	0.5-3.6	5-12
F1-II2	37	2.4	10	ND	ND	0.5	5.1
F1-III3	47	9.4	18	ND	ND	3.4	12
F1-III5	30	5.5	12	ND	ND	1.1	9.7
F1-IV3	33	3.4	13	ND	ND	1.3	8.7

ND: not done

Supplemental Table 3: Platelet kinetic parameters for patient F3-II4

	Parameter value	Reference value
Platelet survival time (days)	4.6	8 - 10
Platelet recovery (% per day)	15	10 - 15
Platelet production rate	0.8 N	NA
Platelet sequestration	Absence	NA

The platelet count at the day of analysis was 128 x 10^9 /L. The injected dose was 2.2 MBq. N: reference value of the laboratory.

References

1. Canault M, Ghalloussi D, Grosdidier C, et al. Human CalDAG-GEFI gene (RASGRP2) mutation affects platelet function and causes severe bleeding. J Exp Med. 2014; 211(7): 1349-1362.
2. Thakur ML, Walsh L, Malech HL and Gottschalk A. Indium-111-labeled human platelets: improved method, efficacy, and evaluation. J Nucl Med. 1981; 22(4): 381-385.
3. Recommended method for indium-111 platelet survival studies. International Committee for Standardization in Hematology. Panel on Diagnostic Applications of Radionuclides. J Nucl Med. 1988; 29(4): 564-566.
4. Lopez RG, Carron C, Oury C, et al. TEL is a sequence-specific transcriptional repressor. J Biol Chem. 1999; 274(42): 30132-30138.
5. Guidez F, Petrie K, Ford AM, et al. Recruitment of the nuclear receptor corepressor N-CoR by the TEL moiety of the childhood leukemia-associated TEL-AML1 oncoprotein. Blood. 2000; 96(7): 2557-2561.
6. Lordier L, Bluteau D, Jalil A, et al. RUNX1-induced silencing of non-muscle myosin heavy chain IIB contributes to megakaryocyte polyploidization. Nat Commun. 2012; 3(717.
7. Naldini L, Blomer U, Gallay P, et al. In vivo gene delivery and stable transduction of nondividing cells by a lentiviral vector. Science. 1996; 272(5259): 263-267.
8. Raslova H, Komura E, Le Couedic JP, et al. FLI1 monoallelic expression combined with its hemizygous loss underlies Paris-Trousseau/Jacobsen thrombopenia. J Clin Invest. 2004; 114(1): 77-84.